

Article

Structural Performance of Modular Sandwich Composite Floor Slabs Containing Basalt FRP-Reinforced Self-Compacting Geopolymer Concrete

Sherin Rahman *, Keerthana John, Bidur Kafle  and Riyadh Al-Ameri 

School of Engineering, Deakin University, Geelong, VIC 3217, Australia; johnke@deakin.edu.au (K.J.); bidur.kafle@deakin.edu.au (B.K.); r.alameri@deakin.edu.au (R.A.-A.)

* Correspondence: skrahman@deakin.edu.au

Abstract: A newly developed innovative steel–geopolymer concrete composite floor slab for use in modular construction is investigated in this study. We present experimental results on the flexural behaviour of eight modular sandwich composite floor slabs with different configurations containing self-compacting geopolymer concrete (SCGC) as infill and Basalt FRP (BFRP) bars as reinforcement. The use of sustainable infill material such as SCGC and non-corrosive BFRP in the proposed composite floor slabs is beneficial from the perspective of environmental sustainability. This study also compares the performance of these composite floor slabs against their hollow counterparts. The overlap between the cells in multi-cell panels acts as additional partitioning walls. The infill material offers the sandwich composite floor slabs significant advantages by improving their load-carrying capacity. A critical analysis of the composite floor slabs for load displacement, failure modes, and strain behaviour is also conducted. The study concludes that the sandwich panels with multiple smaller cells and infill materials exhibit a sound structural performance, reporting a 6–8 times higher load-carrying capacity than their hollow counterparts. A comparison of hollow and infilled panels shows that the infill sandwich panels are suitable as structural slabs. At the same time, the former is more suitable for temporary formworks, shelter, and pedestrian platform applications.

Keywords: basalt FRP; composite floor slabs; modular construction; profiled sheets; sandwich panels; self-compacting geopolymer concrete



Citation: Rahman, S.; John, K.; Kafle, B.; Al-Ameri, R. Structural Performance of Modular Sandwich Composite Floor Slabs Containing Basalt FRP-Reinforced Self-Compacting Geopolymer Concrete. *Appl. Sci.* **2022**, *12*, 4246. <https://doi.org/10.3390/app12094246>

Academic Editors: Rosario Montuori and Muhammad Junaid Munir

Received: 14 March 2022

Accepted: 21 April 2022

Published: 22 April 2022

Publisher's Note: MDPI stays neutral with regard to jurisdictional claims in published maps and institutional affiliations.



Copyright: © 2022 by the authors. Licensee MDPI, Basel, Switzerland. This article is an open access article distributed under the terms and conditions of the Creative Commons Attribution (CC BY) license (<https://creativecommons.org/licenses/by/4.0/>).

1. Introduction

Composite structures gained popularity in the early twentieth century amongst structural engineers [1]. Composite floor slabs made of profiled sheets and concrete have gained greater acceptance. The sheeting is permanent formwork for concrete casting and provides the required tensile reinforcement after the concrete has hardened [2]. Modular construction is highly considered among industry professionals owing to its many advantages such as quality improvement, the enhancement of structural reliability, increased productivity and shortening of construction time, and reduced labour and waste. Likewise, these composite beams' stiffness and bending resistance provide a promising engineering solution. Several studies have investigated the performance of modular slabs by incorporating lightweight composite materials such as fibre-reinforced polymer (FRP), dry board or GFRP sandwich panels [3,4]. These materials generally offer a higher load resistance, leading to increased strength; however, research on their performance in large-scale modular buildings is limited. This has led to the development of steel–concrete composites for the sustainable and efficient construction of modular flooring systems.

New steel–concrete flooring systems have been developed to improve upon the performance of the standard modular flooring system [5]. These also consider Design for Deconstruction (DfD), a significant aspect of sustainability considerations in modular construction [6]. A new deconstructable composite floor system consists of steel framing,

precast concrete planks, and clamping connectors. It is efficient due to conventional composite action and enables refabrication and the reuse of materials [6]. Another system developed for DfD included individual rectangular panels fabricated from thin-gauge steel top and bottom plates with a sandwiched grillage of cold-formed channels and topped with gypsum concrete [7].

The literature also reports double tee, void core slab, half slab, block and beam, sandwich panels and C-formed as the effective forms of precast slab systems [8–13]. In the case of a double tee and void core slab, long spans ranging up to 20 m were studied. However, small-scale, and full-scale specimens of up to eight metres were adopted for the other types of precast slabs. There are limited studies on reinforced concrete composites compared to prestressed and precast slabs [11]. The available studies show that the weight of the floor and partition walls add to the two elements of the heaviest weight in a composite floor module. With an overall restriction on the general dimension and weight of the modules for lifting and transportation, these parameters prove to be critical for modular floor components. Further, these structural slab units do not offer flexibility in terms of geometric parameters such as the width and thickness of the panels, and the spacing, type and size of the sections. Hence, it is important to develop lightweight and resilient structural floor panels that can be designed for the specific needs of the modular unit.

Even with these limitations, a higher volume of studies focusses on the development of steel–concrete infill systems [14], owing to the increase in compressive strength and increased panel stiffness delaying the buckling offered by these composite slabs [15]. Moreover, the profile sheeting provides support by acting as a formwork taking the self-weight of concrete under large spans, avoiding the need for temporary props [16,17]. However, some studies identify that using conventional concrete as an infill material would negatively affect the sustainability aspect of the modular construction concept due to the high amount of carbon emissions associated with the production of Ordinary Portland Cement [18]. A sustainable solution to this is using alternative cementitious materials such as geopolymer concrete, made from fly ash, slag, and other industrial waste products, avoiding using conventional cement [19,20]. Using geopolymer concrete infill in the steel–concrete composite flooring system is advantageous, providing better rigidity to the composite slabs with increased stiffness. Compared to conventional reinforced concrete slabs, it reduces mid-span deflection and the cost of geopolymer concrete preparation [18].

To address the issue of increased self-weight, researchers have also focussed on the use of lightweight concrete using lightweight aggregates or laminated fibres, which reduces the cracks and exhibits a similar structural performance [21]. Lightweight fibres such as Rimix and other polymer fibres offer better interlocking and friction between the sheet–concrete interfaces. Furthermore, the placement of infill material is challenging in closed deck slabs, which creates the need for high-performing composites made of infills such as self-compacting concrete, reducing the labour involvement and cost of compaction [22–24]. Composite slabs made of high-performance engineered composites exhibit better performances than conventional concrete by reducing the number of cracks. The flowable self-compacting infill improves the tensile ductility and strain capacity while maintaining low crack widths [24]. A limited number of studies have been reported in this field of using flowable sustainable concrete despite the advantages of an infill that can fill under its self-weight, reducing time, cost, and labour components [20]. Additionally, in most of the cases, the slab decks have a denser reinforcement which requires the additional use of compacting techniques; however, this study adopts a self-compacting infill material which brings cost savings [20]. A thorough literature review highlights the urgent need to include lightweight, high-strength, and durable materials to maximise the advantages of modular construction.

Thus, in this experimental program, an innovative modular composite floor slab is jointly developed by Deakin University with L2U Pty Ltd., Perth, and FormFlow, Geelong [25]. The study assesses the structural performance and feasibility of using sandwich decks of simple square corrugated sheets [26] with basalt FRP-reinforced self-compacting geopolymer concrete (SCGC) as infill material. This paper presents the test results of the

flexural behaviour of various configurations of the sandwich floor slabs and a detailed analysis and comparison of the load–displacement response, failure modes and load–strain data of the slabs. The performance is then assessed for suitability in modular construction against their hollow counterparts.

2. Materials and Methods

The investigation includes a comprehensive study on previous work by authors and consists of fabricating floor panels from corrugated profile sheets based on the U.S. Patent 8,539,730 B2 [27] and later infilling them with self-compacting geopolymer concrete (SCGC) to act as a composite slab. Three different configurations of floor slabs containing SCGC infill with a single cell (SC), double cell (DC) and triple cell (TC) were investigated, similar to the previous study by the authors on hollow floor panels [28].

2.1. Panels for Modular Composite Slabs

Modular composite slabs from simple square profiled corrugated sheets of 0.42 mm thickness were fabricated, which is explained in detail in the previous work by the authors [28]. Trapezoidal corrugated sheets were bent and folded along slots to form individual hollow cellular panels for infilling with SCGC. The overall cross-section details of such panels are presented in Figure 1.

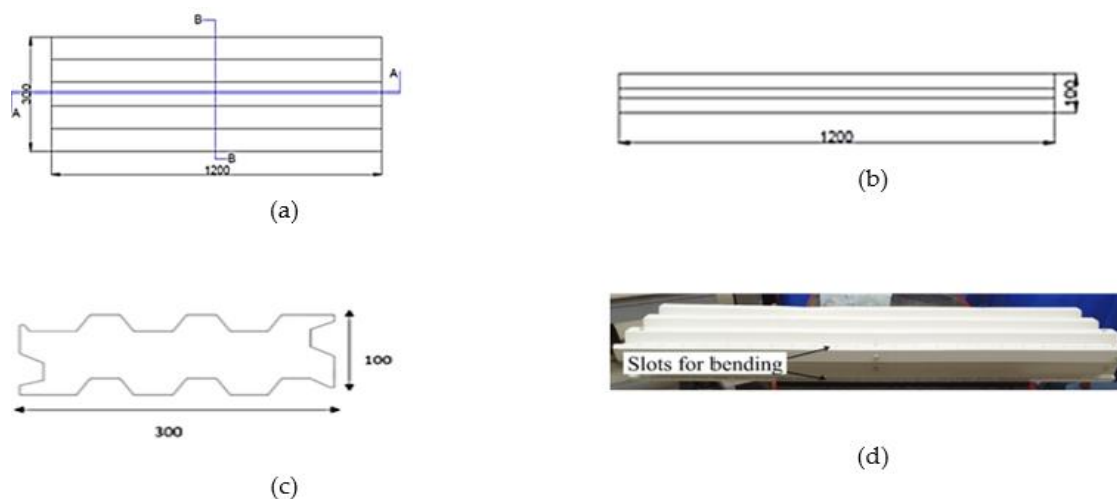


Figure 1. Overall dimensions of panel: (a) top view of the panel; (b) cross-section A-A; (c) cross-section B-B; (d) sample panels with a slot along the bents.

The current study investigates three different cell configurations of the composite floor slabs. Single-cell, double-cell and triple-cell slabs are fabricated to assess and compare the performance of each configuration (Figure 2). The overall dimensions were kept uniform with 1200 mm length (L), 300 mm width (W), and 100 mm depth (D).

2.2. Infill Material for Composite Floor Slabs

The self-compacting geopolymer concrete (SCGC) recently developed by the engineering team at Deakin University [18] was used as the primary infill material in this study. Due to the corrugated nature of test slabs, a flowable type of concrete allows better placement without the use of vibrators. The SCGC infill is self-compacting and flowable in nature, which facilitated the casting and placing of the infill into the slab specimens without any additional equipment requirements for compaction. Figure 3 shows the pouring of infill SCGC and casting of composite floor slabs.

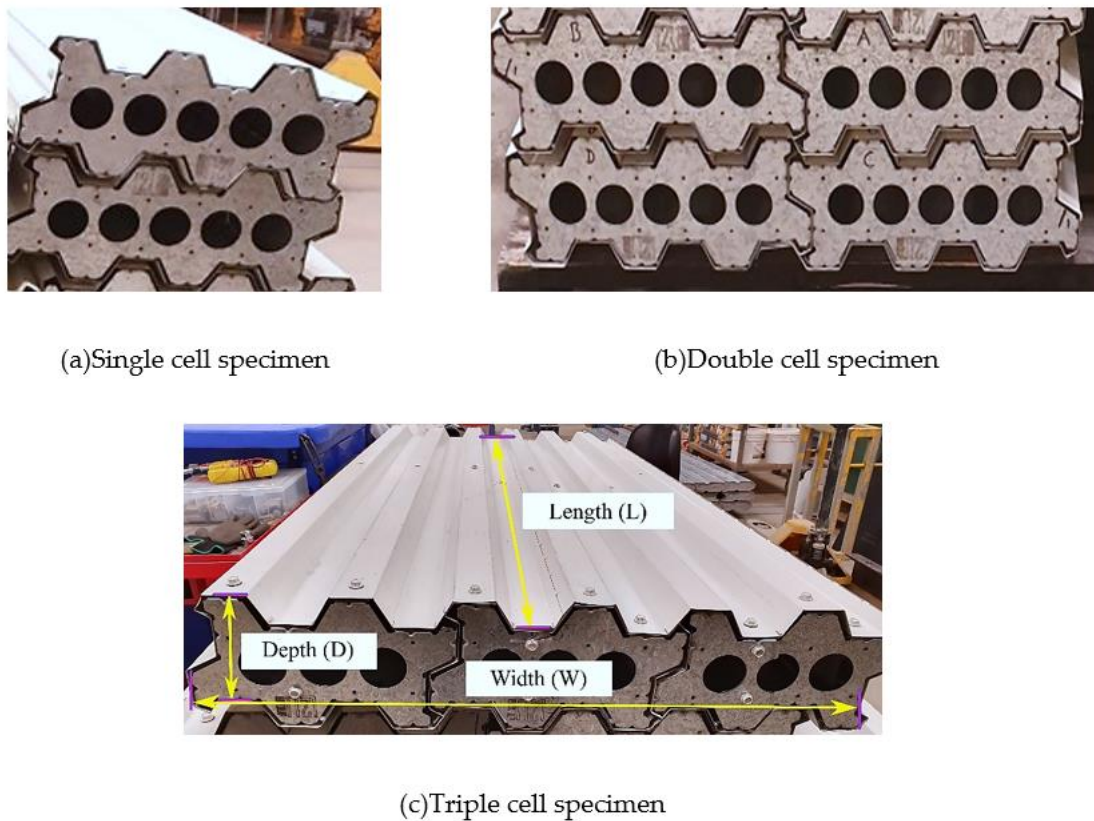


Figure 2. Specimen types.



Figure 3. Casting of panels.

SCGC used in this study is a zero-cement, flowable mix made from industrial combustion waste products, including fly ash, micro-fly ash and slag. The geopolymer concrete mix attains its cementitious properties and a design compressive strength of 40 MPa at 28 days of ambient curing by adding sodium metasilicate. The binder materials, alkali activator (anhydrous sodium metasilicate), and the aggregates (coarse gravel and fine sand) were sourced from local suppliers in Australia. Furthermore, another infill material that contained the original self-compacting geopolymer mix added with chopped basalt fibres (1% by weight of the total binders in the SCGC mix) was also used in this study. The details

of the SCGC mix and the amount of chopped basalt fibres used as the infill material are given in Table 1 [29]:

Table 1. Mix proportion of self-compacting geopolymer concrete along with chopped basalt fibre content.

Mix Proportion (kg/m ³)	
Fly Ash	480
Slag	360
Micro-Fly Ash	120
Sodium metasilicate (Anhy.) Alkali Activator	96
Fine Aggregate	763
Coarse Aggregate	677
Chopped Basalt fibres	10.56

The addition of short fibres is proven to reduce the shrinkage cracks in the infill slab [30]. The addition of chopped basalt fibres of 12 mm length reduces the early cracks in self-compacting concrete mixes, which enhances the performance of the test specimens [31].

Furthermore, the floor panels are reinforced with non-corrosive Basalt FRP (BFRP) bars to provide the required flexural strength and satisfy the design requirements. These BFRP bars and the basalt fibres were sourced from Beyond Materials, Australia [32]. All the composite slab specimens were reinforced with BFRP bars of 8 mm diameter at 100 mm spacing as per the ACI 440.1R-15 design requirements [33]. The combination of self-compacting geopolymer concrete with BFRP reinforcing bars is a sustainable, environmentally friendly, and durable alternative against the conventional steel–concrete reinforced structures. The use of BFRP bars replacing the traditional steel reinforcing bars will help to reduce the overall weight of the test specimen and provide protection against corrosion in addition to the higher tensile strengths.

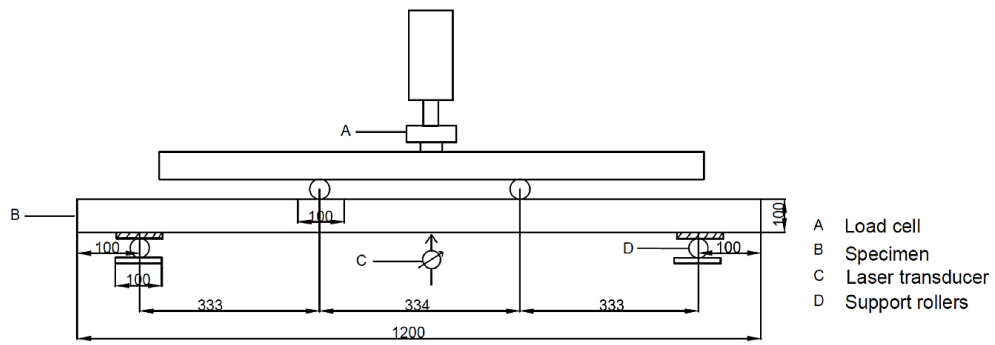
The total number of test specimens and the type of infill adopted for this experimental testing program is detailed in Table 2. The influence and nature of the performance of chopped basalt fibre containing infill slabs are confirmed by single- and double-cell panels. Hence, the experiment was optimised without including chopped basalt fibres in the triple-cell configuration.

Table 2. Details of panels for testing.

Sample Type	Panel Dimensions (L × W × D) mm	Width of Individual Cell (W) mm	Number of Samples	
			SCGC + BFRP Bars	SCGC + BFRP Bars + Chopped Basalt Fibre
Single cell with infill	1200 × 300 × 100	300	1	2
Double cell with infill	1200 × 600 × 100	300	2	1
Triple cell with infill	1200 × 600 × 100	200	2	-
Total number of specimens			8	

2.3. Test Set-Up

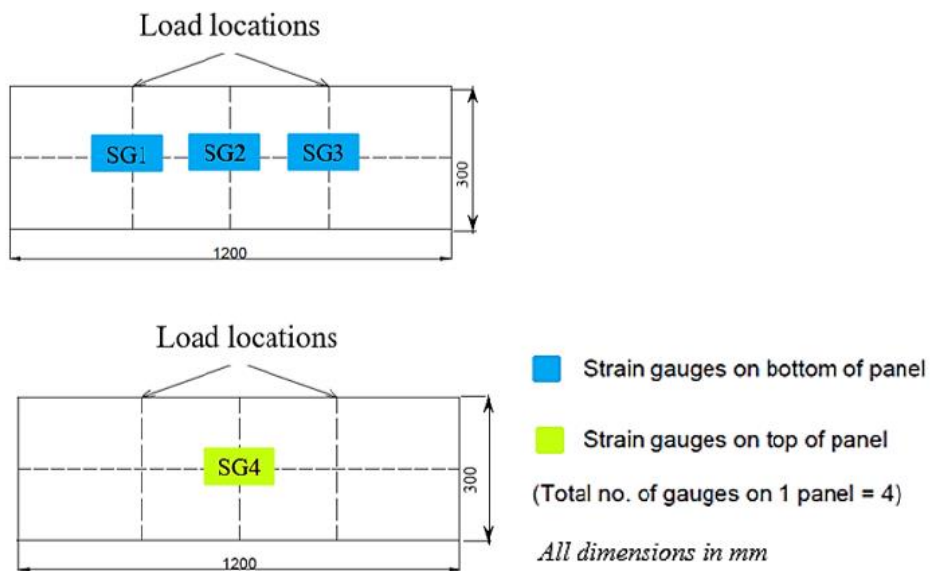
A four-point bending test was conducted on the infill composite floor slabs where the specimens had an effective span of 1000 mm, and the four -point bend test set-up and arrangement is shown in Figure 4a,b. The load was applied to the centre using a 500 kN capacity load frame, maintaining a displacement rate of 2.5 mm/min. The mid-point displacement was recorded using a laser transducer underneath the panel. Four strain gauges were placed on the panel, with three on the bottom side and one on the top of the panel to measure the strain data, as seen in Figure 4c. A data acquisition system connected to the load frame controls was programmed to measure the load, displacement, and strain data.



(a) Four Point Bend test details



(b) Test arrangement of single-cell panel



(c) Position of strain gauges

Figure 4. Test set-up details.

3. Result and Discussion

3.1. Load–Displacement Behaviour

3.1.1. Single-Cell Panels with Infill

The load–displacement behaviour of the single-cell panels is shown along with ultimate load, and the gradual yield in Figure 5. The single cells with both types of infill material, namely SCGC and SCGC containing chopped basalt fibre, reported a gradual drop post the peak load, showing a ductile performance. The peak loads attained by all the single-cell specimens were in the range of 40 kN. However, the single cell with fibres recorded a slightly higher ultimate load-carrying capacity at an average of 42.22 kN. This signifies that the chopped basalt fibres have contributed to the load-carrying capacity of the panels by improving their ductility. The displacement is also higher at the ultimate load in a single cell with no fibres.

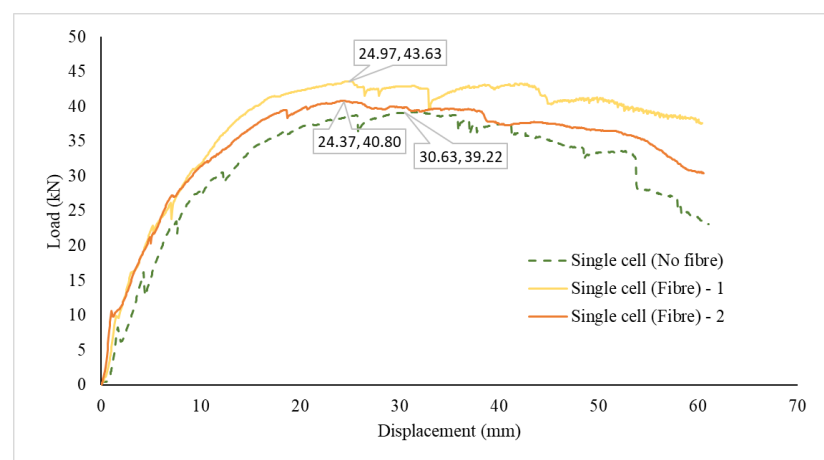


Figure 5. Load vs. displacement of single-cell infill panels.

Again, from the load–displacement curves, it can be seen that there were more flexural cracks in the infill panels without chopped basalt fibres, which is highlighted by the presence of several irregularities due to load drops in the plot. However, a smoother load increase due to the chopped basalt fibres was observed in the other panels. This demonstrates that chopped basalt fibres positively contribute to reducing cracks on floor slabs. The averaged results of the single-cell test specimens are tabulated in Table 3.

Table 3. Results of single-cell composite floor slabs.

Sample Type	Sample Designation	Infill Type	Ultimate Load (kN)	Displacement (mm)
Single cell	Single cell (Fibre)	SCGC + BFRP + Chopped Basalt fibre	42.22	24.70
Single cell	Single cell (No fibre)	SCGC + BFRP	39.22	30.63

3.1.2. Double-Cell Panels with Infill

Figure 6 shows the ultimate load, yield phase, and the load–displacement behaviour of the double-cell specimens, and the average test results are compiled in Table 4. The load–displacement curves for the double cells report a similar trend as that of single-cell panels but with a higher load-carrying capacity. It is noted that the infill panels containing chopped basalt fibres reported a slight increase in ultimate loads due to the improved impact strength offered by the randomly dispersed chopped basalt fibres, enhancing the tensile properties of the SCGC matrix. However, the average peak load of both infill types was 72 kN, which is a 44% increase compared to the single-cell panel specimens. The increase in load capacity for the double cells can be attributed to the overlap between each

cell panel, which leads to a higher stiffness across the panel cross-section, leading to a better load distribution in the slab.

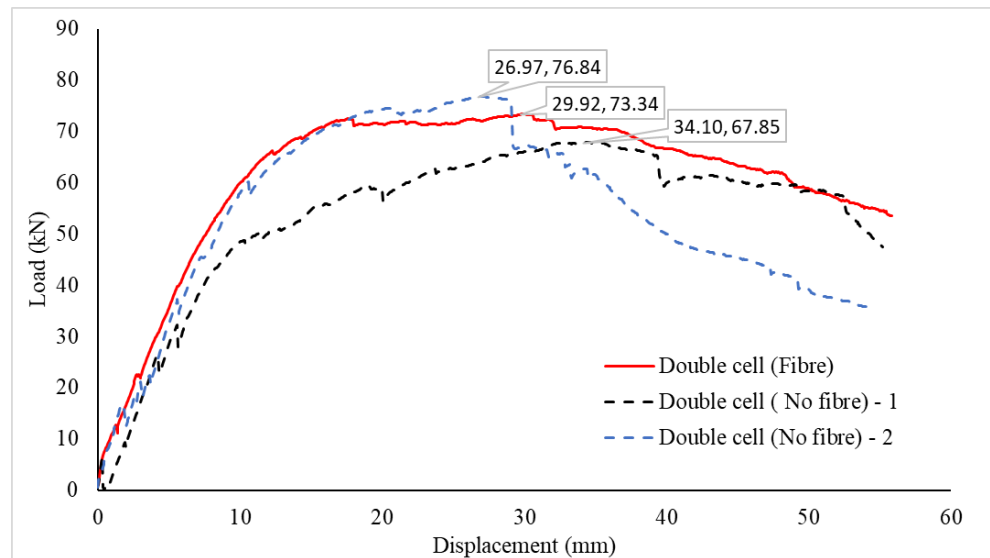


Figure 6. Load vs. displacement of double-cell infill panels.

Table 4. Results of double-cell composite slabs.

Sample Type	Sample Designation	Infill Type	Ultimate Load (kN)	Displacement (mm)
Double cell	Double cell (Fibre)	SCGC + BFRP + Chopped Basalt fibre	73.34	29.92
Double cell	Double cell (No fibre)	SCGC + BFRP	72.35	30.71

3.1.3. Triple-Cell Panels with Infill

The load–displacement relationship of triple-cell panels is shown in Figure 7, reporting an average ultimate load of 98.15 kN. The ultimate load of the triple-cell specimen is also tabulated in Table 5. It is shown that the addition of any number of cells to the panels improves the load-carrying capacity of the floor slabs proportionally. This is mainly attributed to the overlap at the side of each cell. It is worth noting that the double- and triple-cell specimens have the same overall width of 600 mm, with a length of 1200 mm. The only difference is the additional partitioning, which led to a 35.6% increase in the load-carrying capacity. The influence of chopped basalt fibres in infill material for panels has been well established from the tests of single- and double-cell panels. Hence, the triple-cell panels were both tested without fibres.

Table 5. Results from triple-cell infill panels.

Sample Type	Sample Designation	Infill Type	Ultimate Load (kN)	Displacement (mm)
Triple cell	Triple cell (No fibre)	SCGC + BFRP	103.77	35.35
Triple cell	Triple cell (No fibre)	SCGC + BFRP	92.53	27.77

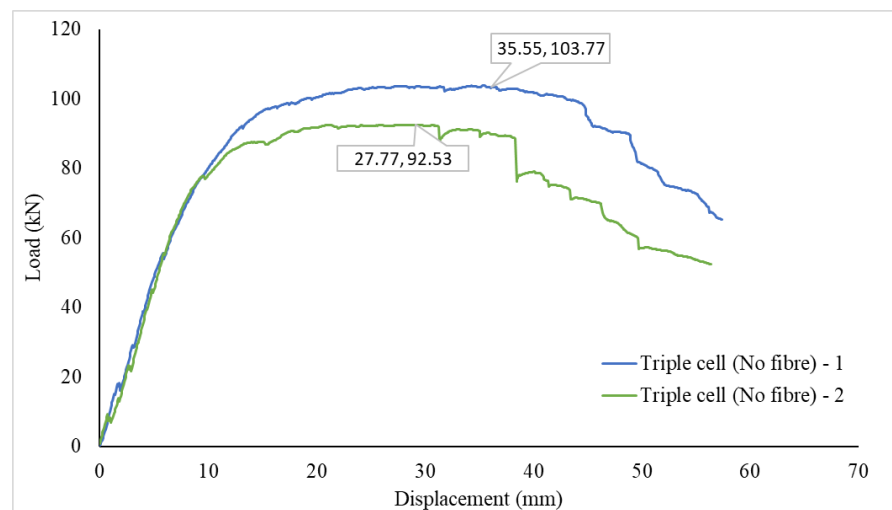
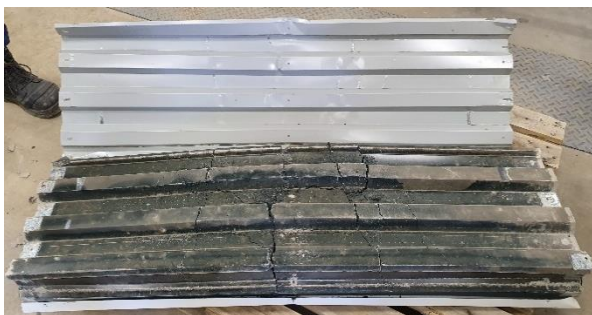


Figure 7. Load vs. displacement of triple-cell infill panels.

3.2. Failure Mode

3.2.1. Single-Cell Panels with Infill

The primary failure mode in single-cell panels was flexure failure, and flexure cracks were also noticed under the loading points and at the centre of the panel (Figure 8a). This was initiated by buckling sheets at the edge, as seen in Figure 8b, which was followed by tearing the sheets at the slots, as seen in Figure 8c. The sheet was also seen to debond at the free end without the endplate and lose its integrity of shape (Figure 8d). This behaviour resulted in a slip of 1.4 mm between the concrete and steel at this end (Figure 8e). The panels were opened after testing to investigate the cracks in concrete. The load–displacement curve also translates the failure of sheets and the corresponding formation of cracks in concrete. Similar behaviours were seen for all panels without fibres. However, fewer cracks were noticed in panels with chopped basalt fibres due to their ductility, resulting in crack reduction.



(a) Opened sample—Flexure cracks on the bottom surface



(b) Buckling of the sheet

Figure 8. Cont.



(c) Tearing of sheet



(d) Sheet debonding at edges



(e) Slip of concrete at the free end

Figure 8. Failure modes of single-cell panels.

3.2.2. Multi-Cell Panels with Infill

The multi-cell panels, including double and triple cells, underwent flexure failure, similar to single-cell panels. All the configurations of multi-cell panels recorded identical modes of failure. The common failures observed were tearing of the sheet (Figure 9a), debonding at the edges of the panel (Figure 9b) and local buckling (Figure 9c). The slots for bending the sheets widened at higher displacements, eventually tearing at the ends. At higher displacements, the decking sheets started to stretch, leading to the flattening of the sheets at the corners of the slab and debonding at the edges of the panel. The geopolymer concrete experienced flexural cracks underneath the loading points and panel centre (Figure 9d). However, no separation between the cells of the multi-cell panels was observed. This behaviour indicates that the overlap works as a good load-carrying component.



(a) Tearing of sheet



(b) Sheet debonding at edges

Figure 9. Cont.



(c) Local buckling of the sheet



(d) Flexure cracks

Figure 9. Failure mode of multi-cell panels.

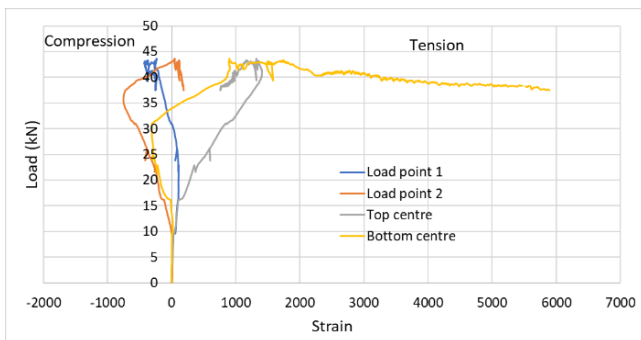
3.3. Strain Mapping

3.3.1. Single-Cell Panels with Infill

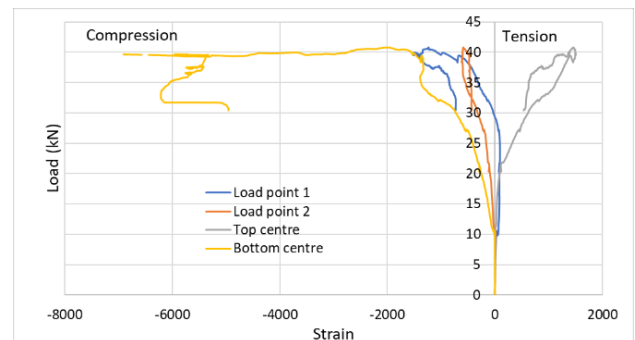
The measured strain values against the applied load for single-cell panels with chopped basalt fibres in the infill material are shown in Figure 10. It was found that the top skin remained in compression. In contrast, the bottom skin moved from tension to compression in the second sample, which could be due to the local buckling of the bottom skin, as shown in Figures 10 and 11a.



Figure 10. Compression in bottom skin due to buckling.



(a) Single cell (Fibre) - (1)



(b) Single cell (Fibre) - (2)

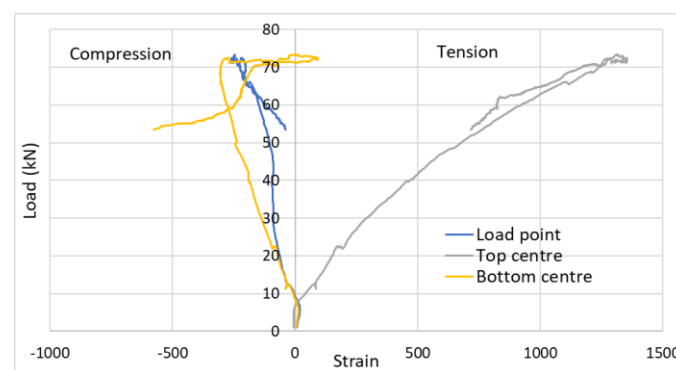
Figure 11. Strain mapping of single-cell panels with chopped basalt fibres.

The bottom skin of the steel sheet remained in tension in the first specimen (Figure 11b). It was observed that the bottom skin had the most significant strain values, suggesting that the tensile property of the steel sheeting was sufficiently utilised in these panels. The strain under the load points remained relatively low, and minor variations at points of local buckling or deformations occurred on the steel. The strain mapping details indicate the improved ductile performance of the single-cell panels due to the presence of additional fibres in the infill material.

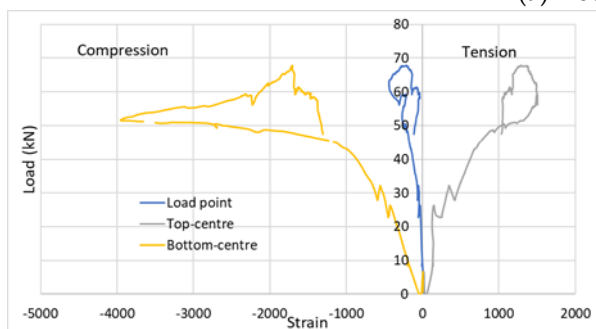
3.3.2. Multi-Cell Panels with Infill

Double-Cell Panels with Infill

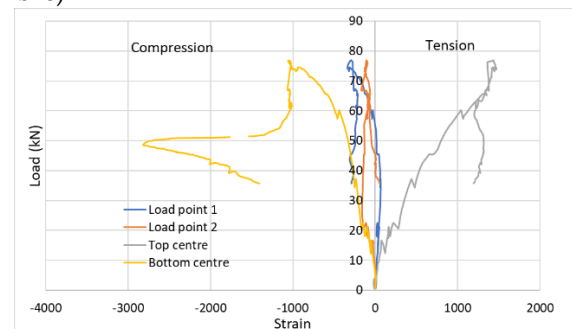
The strain mapping of the double-cell panels is shown in Figure 12. All the panels show that with an increase in loading, the mid-span of the bottom skin remained in compression, and the top skin remained in tension. In double-cell panels without fibres, a deviation in the curves was noticed when the panels underwent local buckling or tearing of sheets, which resulted in a drop in the strain value. The strain in the bottom skin of the double-cell panel with chopped basalt fibres was less than in the panels without them. It showed fewer variations due to the SCGC concrete combined with the chopped basalt fibres making the panels more ductile. No sudden or brittle failure was reported for the panels containing chopped basalt fibres in the infill. The strain mapping data of double cells with fibre indicates that the tensile properties of the deck were not completely utilised since the steel sheeting failed before the yield values of strain. However, double cells without fibre sufficiently utilised the full tensile capacity of the deck panels to attain the ultimate load.



(a) Double cell (Fibre)



(b) Double cell (No fibre) - (1)



(c) Double cell (No fibre) - (2)

Figure 12. Strain mapping of double-cell panels.

Triple-Cell Panels with Infill

The two triple-cell panels tested without chopped basalt fibres showed similar behaviours, as presented in Figure 13. The top skin was in tension, and the bottom in compression. However, close to the ultimate load, when the cracks in concrete began widening, and the steel and concrete interface began to slip, a variation in the strain data on

the bottom skin was noticed. The strain reduced and moved away from compression until the panel failed at the ultimate load. This also indicates that the neutral axis moved into the steel sheeting and part of the steel resisted the compression. The top skin yielded first and did not take any more load, whereas the bottom skin continued taking a steady amount of load after reaching the ultimate load until complete failure occurred. The strain mapping data depict that the strain values in tension reported lower values than those of the yield strength of steel sheets, indicating that the full capacity of the steel deck was not utilised.

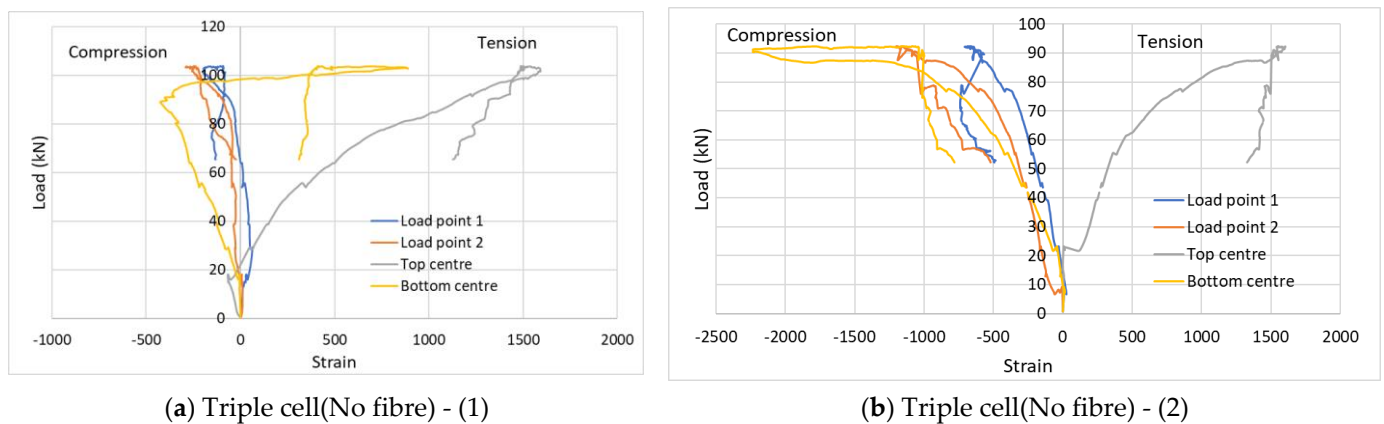


Figure 13. Strain mapping of triple-cell panels.

3.4. Comparison with the Previous Study

From the current experimental results, it can be concluded that any addition of cells significantly improves the load-carrying capacity of the proposed floor slab panels. This is attributed to the presence of overlapped sheets between individual cell panels. Triple-cell panels have the highest ultimate load while having the same width and length as double-cell panels. Fibres improve the ductility of the panels and offer a comparatively better load capacity than panels without any fibres. The primary failure noticed in all panels is flexural failure. This failure is initiated by the buckling and tearing of the steel sheets, and then the cracking of the geopolymer concrete.

To further understand and highlight the role of infill material, a detailed comparison of the test results is presented against a similar study by the authors on composite floor panels without infill [28]. Thus, the performance of single- (SC), double- (DC), and triple-cell (TC) panels with and without infill were evaluated in terms of ultimate load capacity and failure mode for all test specimens.

3.4.1. Comparison of Ultimate Load Capacity

This section compares the ultimate load capacity of the various panel configurations. It is confirmed that the addition of infill material significantly improves the load capacity of the panel to act as a structural component in modular construction. The load capacity of the hollow panels was in the range of 6 kN to 13 kN (single-cell to multi-cell panels), which can be safely adapted for temporary flooring applications such as formworks and in temporary housing, such as refugee shelters, as floors according to the AS 2327–2017 standard code [34]. Considering the floor slabs with SCGC infill and reinforcement, the ultimate load ranged between 39 kN and 98 kN (single-cell to multi-cell slabs), which shows a significant increase, highlighting their potential as structural floor slabs.

It can be seen in Figure 14 that a hollow single-cell floor panel reported only a 6 kN ultimate load, which, when filled with SCGC reinforced in BFRP, reported a six-fold increase in the ultimate load capacity. Moreover, the SCGC with chopped basalt fibre reinforced in BFRP reported a further 7% increase in the ultimate load for single-cell floor panels compared with samples without chopped basalt fibre additions with better ductility. A double-cell hollow panel reported an ultimate load of 8.59 kN which is eight times higher

when filled with SCGC, chopped basalt fibres, and BFRP bars. This shows the relevance of infill material in improving structural performance. A similar trend was reported by triple-cell panels, where the ultimate load was increased seven-fold, reporting a peak load of 98 kN for panels with infill.

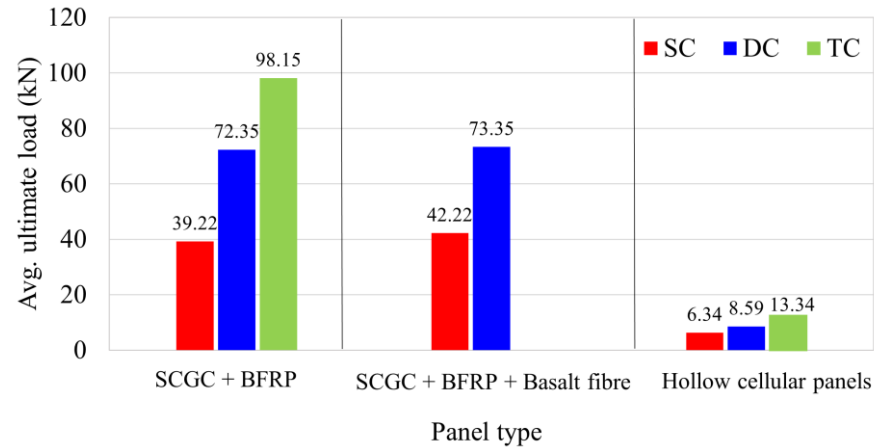


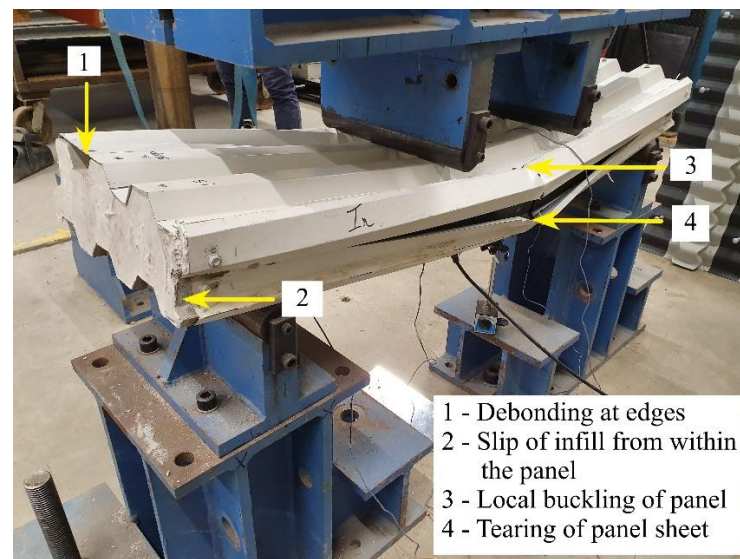
Figure 14. Summary of ultimate load capacity of various configurations of test panels.

In summary, the presence of infill material significantly improves the performance of these panels for advanced modular slab systems. Along with the improvement in load capacity, the presence of an infill material offers a significant increase in ductility and stiffness properties.

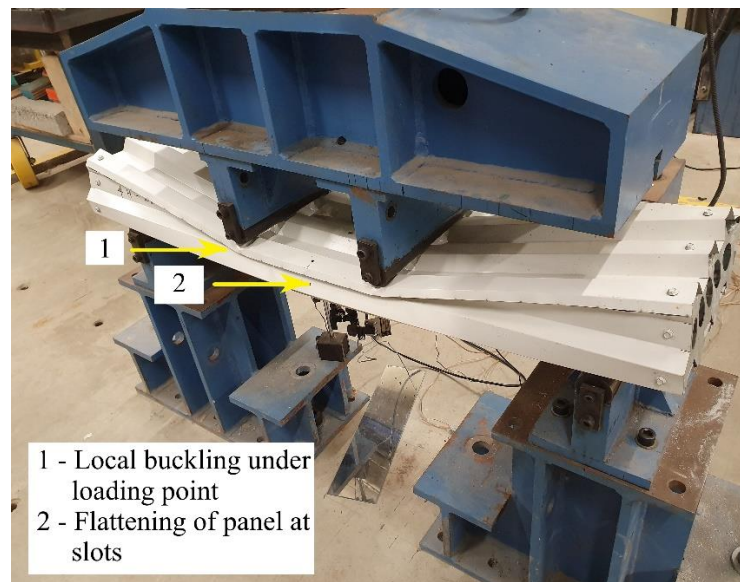
3.4.2. Comparison of Failure Mode

A comparison of the failure modes of different configurations of multi-cell and single-cell panels was also carried out for panels with and without infill. It was found that local buckling was the primary failure mode in hollow cell panels irrespective of the cell number. However, there was limited buckling under the loading points for the infill panels. The infill panels reported tearing and debonding of the sheet corners due to the slippage of hardened infill material from the steel in the panels during the test, which was not the case for the hollow panels. Despite wear and tear on the sheet surface, a significant load was transferred and held by the concrete until the flexural failure of the slab specimens containing SCGC infill. Major failure modes observed in infill panels and panels without infill are highlighted in Figure 15.

Furthermore, an immediate buckling and thereby failure of the panel specimens were observed in the hollow single-cell panels due to a lack of effective load transfer between the top and bottom skins. Moreover, there was no separation between the individual cells in both hollow and infill multi-cell panels, indicating that the overlap of the sheets at each cell joint plays a significant role in the structural integrity of the specimens and, thereby, efficient load distribution. It is implied that infill material such as the SCGC has assisted the efficient load transfer between top and bottom skins, thereby offering higher load resistance and preventing the premature failure of the panel specimens.



(a) Failure modes in panels with infill



(b) Failure modes in hollow panels without infill

Figure 15. Comparison of failure modes in panels with and without infill.

4. Conclusions

Various configurations of floor panels, including single-cell, double-cell, and triple-cell panels with SCGC infill, were assessed, considering structural performance, for use as flooring systems. Self-compacting geopolymer concrete was used as the infill material, and BFRP bars were used for reinforcement. Chopped basalt fibres were employed as an alternative in the infill to improve the properties of the flooring components. Due to the novelty in the panel configuration, the use of infill materials proves to be a promising contribution to modular construction components, especially for use as structural flooring applications in emergency housing sectors. The results were also compared with a similar study by the authors on composite floor panels without infill.

The following main conclusions from the results are derived:

1. Sandwich panels with a greater number of cells of smaller size were found to offer increased load-carrying capacity and stiffness than the single-cell panels due to the presence of overlapping sheets.

2. The addition of chopped basalt fibres in SCGC improves the durability of the sandwich panels, with a 7% increase in the load-carrying capacity and reduction in crack intensity.
3. Flowable SCGC proved to be an effective infill option for complex composite deck arrangements, offering ease in placement without vibrators.
4. The single-cell panels containing infill material offered a minimum of a 6-fold increase in ultimate load capacity in comparison to its hollow counterpart, and the load capacity increased by 8-fold as the cell numbers increased.
5. Providing an infill material modifies these sandwich composite floor slabs into a structural component that can be used in modular construction.
6. Future research can compare infill materials in these panels and assess commercial use marketability, economic, thermal performance, and sustainability quotients.

Author Contributions: Conceptualization, R.A.-A. and B.K.; methodology, S.R., K.J., B.K. and R.A.-A.; formal analysis, S.R., and K.J.; investigation, S.R. and K.J.; writing—original draft preparation, S.R. and K.J.; writing—review and editing, B.K. and R.A.-A.; supervision, B.K. and R.A.-A.; project administration, B.K. and R.A.-A.; funding acquisition, R.A.-A. All authors have read and agreed to the published version of the manuscript.

Funding: The authors acknowledge the research fund from Deakin University, Victoria, Australia. In addition, the authors acknowledge the kind support by industry partners L2U Pty. Ltd. and FormFlow, Australia.

Institutional Review Board Statement: Not applicable.

Informed Consent Statement: Not applicable.

Data Availability Statement: The data presented in this study are available on request from the authors.

Acknowledgments: The authors acknowledge the technical support by the industry partners L2U Pty. Ltd., Beyond Materials Pty. Ltd., and FormFlow, Australia. The authors also acknowledge gratefully the support and guidance offered by Klaus Hansen-Director, L2U Group Pty. Ltd., Mohamed Elchalakani- Senior Lecturer, University of Western Australia, Matthias Weiss—Senior Research Fellow, Institute for Frontier Materials, Reza Hosseini—Associate Head of School, Deakin University, and Nilupa Udawatta—Senior Lecturer, Deakin University. The authors are grateful for the laboratory assistance provided by the Technical Staff—Lube Veljanoski and Michael Shanahan to complete the experimental investigation at the Structures Laboratory, Deakin University.

Conflicts of Interest: The authors declare no conflict of interest.

Abbreviations

BFRP	Basalt FRP
DC	Double Cell
D	Depth
DfD	Design for Deconstruction
FRP	Fibre-Reinforced Polymer
GFRP	Glass Fibre-Reinforced Polymer
L	Length
SC	Single Cell
SCGC	Self-Compacting Geopolymer Concrete
TC	Triple Cell
W	Width

References

1. Nie, J.; Wang, J.; Gou, S.; Zhu, Y.; Fan, J. Technological development and engineering applications of novel steel-concrete composite structures. *Front. Struct. Civ. Eng.* **2019**, *13*, 1–14. [[CrossRef](#)]
2. Mäkeläinen, P.; Sun, Y. The longitudinal shear behaviour of a new steel sheeting profile for composite floor slabs. *J. Constr. Steel Res.* **1999**, *49*, 117–128. [[CrossRef](#)]
3. Hamid, A.A.; Wan Badaruzzaman, W.H. Performance of Infilled Profiled Steel Sheet Dry Board PSSDB Load Bearing Wall. *Int. J. Eng.* **2004**, *17*, 343–348.

4. Satasivam, S.; Bai, Y.; Zhao, X.-L. Adhesively bonded modular GFRP web-flange sandwich for building floor construction. *Compos. Struct.* **2014**, *111*, 381–392. [[CrossRef](#)]
5. O'Hegarty, R.; Kinnane, O. Review of precast concrete sandwich panels and their innovations. *Constr. Build. Mater.* **2020**, *233*, 117145. [[CrossRef](#)]
6. Wang, L.; Webster, M.D.; Hajjar, J.F. Behavior of Deconstructable Steel-Concrete Shear Connection in Composite Beams. *Struct. Congr.* **2015**, *2015*, 876–887.
7. Boadi-Danquah, E.; Robertson, B.; Fadden, M.; Sutley, E.J.; Colistra, J.; De Temmerman, N.; Brebbia, C.A. Lightweight modular steel floor system for rapidly constructible and reconfigurable buildings. *Int. J. Comput. Methods Exp. Meas.* **2017**, *5*, 562–573. [[CrossRef](#)]
8. Naito, C.; Cao, L.; Peter, W. Precast concrete double-tee connections, part 1: Tension behavior. *PCI J.* **2009**, *54*, 49–66. [[CrossRef](#)]
9. Cao, L.; Naito, C. Precast concrete double-tee connectors, part 2: Shear behavior. *PCI J.* **2009**, *54*, 97. [[CrossRef](#)]
10. Brunesi, E.; Nascimbene, R. Numerical web-shear strength assessment of precast prestressed hollow core slab units. *Eng. Struct.* **2015**, *102*, 13–30. [[CrossRef](#)]
11. Lee, J.D.; Yoon, J.K.; Kang, T.H.-K. Combined half precast concrete slab and post-tensioned slab topping system for basement parking structures. *J. Struct. Integr. Maint.* **2016**, *1*, 1–9. [[CrossRef](#)]
12. Pavic, A.; Miskovic, Z.; Zivanovic, S. Modal properties of beam-and-block pre-cast floors. *IES J. Part A Civ. Struct. Eng.* **2008**, *1*, 171–185. [[CrossRef](#)]
13. Amran, Y.H.M.; Rashid, R.S.M.; Hejazi, F.; Ali, A.A.A.; Safiee, N.A.; Bida, S.M. Structural Performance of Precast Foamed Concrete Sandwich Panel Subjected to Axial Load. *KSCE J. Civ. Eng.* **2018**, *22*, 1179–1192. [[CrossRef](#)]
14. Karimipour, A.; Ghalehnovi, M.; Golmohammadi, M.; de Brito, J. Experimental Investigation on the Shear Behaviour of Stud-Bolt Connectors of Steel-Concrete-Steel Fibre-Reinforced Recycled Aggregates Sandwich Panels. *Materials* **2021**, *14*, 5185. [[CrossRef](#)]
15. Jaffar, M.I.; Badaruzzaman, W.H.W.; Abdullah, M.A.B.; Baharom, S.; Moga, L.; Sandu, A.V. Relationship between panel stiffness and mid-span deflection in Profiled steel sheeting dry board with geopolymer concrete infill. *Mater. Plast.* **2015**, *52*, 243–248.
16. Sutiman, N.A.; Majid, M.; Jaini, Z.; Roslan, A. State of Art on Steel Composite Slab Systems. *Recent Trends Civ. Eng. Built Environ.* **2020**, *1*, 28–54.
17. John, K.; Ashraf, M.; Weiss, M.; Al-Ameri, R. Experimental Investigation of Novel Corrugated Steel Deck under Construction Load for Composite Slim-Flooring. *Buildings* **2020**, *10*, 208. [[CrossRef](#)]
18. Jaffar, M.I.; Badaruzzaman, W.H.W.; Abdullah, M.M.A.B.; Kamarulzaman, K.; Seraji, M. Effect of Geopolymer Concrete Infill on Profiled Steel Sheeting Half Dry Board (PSSHDB) Floor System Subjected to Bending Moment. *Appl. Mech. Mater.* **2015**, *754–755*, 354–358. [[CrossRef](#)]
19. Jaffar, M.I.; Badaruzzaman, W.H.W.; Baharom, S. Experimental Tests on Bending Behavior of Profiled Steel Sheeting Dry Board Composite Floor with Geopolymer Concrete Infill. *Lat. Am. J. Solids Struct.* **2016**, *13*, 272–295. [[CrossRef](#)]
20. Rahman, S.K.; Al-Ameri, R. A newly developed self-compacting geopolymer concrete under ambient condition. *Constr. Build. Mater.* **2021**, *267*, 121822. [[CrossRef](#)]
21. Li, X.; Zheng, X.; Ashraf, M.; Li, H. The longitudinal shear bond behavior of an innovative laminated fiber reinforced composite slab. *Constr. Build. Mater.* **2019**, *215*, 508–522. [[CrossRef](#)]
22. Pang, S.D.; Liew, J.Y.R.L.; Dai, Z.; Wang, Y. Prefabricated Prefinished Volumetric Construction Joining Techniques Review. In Proceedings of the Modular and Offsite Construction (MOC) Summit, Edmonton, AB, Canada, 29 September–1 October 2016.
23. Liew, J.Y.R.; Chua, Y.S.; Dai, Z. *Steel Concrete Composite Systems for Modular Construction of High-Rise Buildings, Structures*; Elsevier: Amsterdam, The Netherlands, 2019; pp. 135–149.
24. Hossain, K.; Attarde, S.; Anwar, M. Finite element modelling of profiled steel deck composite slab system with engineered cementitious composite under monotonic loading. *Eng. Struct.* **2019**, *186*, 13–25. [[CrossRef](#)]
25. FormFlow. 2020. Available online: <https://formflow.net.au> (accessed on 12 March 2020).
26. Lysaght Australia. 2021. Available online: <https://cdn.dcs.lysaght.com/download/lysaght-build-on-inspiration-design-in-steel> (accessed on 1 June 2021).
27. Madsen, T.; Hansen, K.H. Building System. US Patent 8,539,730, 24 September 2013.
28. John, K.; Rahman, S.; Kafle, B.; Weiss, M.; Hansen, K.; Elchalakani, M.; Udawatta, N.; Hosseini, M.R.; Al-Ameri, R. Structural Performance Assessment of Innovative Hollow Cellular Panels for Modular Flooring System. *Buildings* **2022**, *12*, 57. [[CrossRef](#)]
29. Rahman, S.; Al-Ameri, R. Experimental Investigation and Artificial Neural Network Based Prediction of Bond Strength in Self-Compacting Geopolymer Concrete Reinforced with Basalt FRP Bars. *Appl. Sci.* **2021**, *11*, 4889. [[CrossRef](#)]
30. Abed, F.; AlHafiz, A.R. Effect of basalt fibers on the flexural behavior of concrete beams reinforced with BFRP bars. *Compos. Struct.* **2019**, *215*, 23–34. [[CrossRef](#)]
31. Adesina, A. Performance of cementitious composites reinforced with chopped basalt fibres—An overview. *Constr. Build. Mater.* **2021**, *266*, 120970. [[CrossRef](#)]
32. Beyond Materials Pty. Ltd. 2021. Available online: <https://basaltfrp.com.au/> (accessed on 1 January 2022).
33. American Concrete Institute, *Guide for the Design and Construction of Structural Concrete Reinforced with Fiber-Reinforced Polymer (FRP) Bars (ACI 440.1R-15)*; American Concrete Institute: Farmington Hills, MI, USA, 2015.
34. AS:2327-2017; Composite Structures—Composite Steel-Concrete Construction in Buildings; Standards Australia: Sydney, NSW, Australia, 2017.